第34卷第11期 焊 接 学 报 Vol. 34 No. 11
2013年11月 TRANSACTIONS OF THE CHINA WELDING INSTITUTION November 2013

Cu-P 变质对 Al-Si-Zn 钎料钎缝组织的影响

戴 玮[1]， 薛松柏[1]， 孙 波[2]， 娄 江[2]， 王水庆[2]
(1. 南京航空航天大学 材料科学与技术学院，南京 210016; 2. 浙江新锐焊接材料有限公司，嵊州 312452)

摘 要：研究了 Cu-P 合金变质对 Al-Si-Zn 钎料 6061 铝合金钎缝组织及性能的影响. 结果表明，Cu-P 变质能提高 Al-Si-Zn 钎料接头的抗拉强度，并且在 Cu-P 合金添加量为 1.5% 时达到最大值 144 MPa. P 元素的加入不仅能变质初晶硅及共晶硅，还能细化钎料基体. 变质后的钎料合金中，初晶硅以 AlP 为衬底生长，使得初晶硅明显细化，同时磷的加入使得 Al-Si 共晶点偏移，初晶硅数量增多. 变质前后的两种钎料的 6061 铝合金钎焊接头微观组织分析结果表明，Al-Si-Zn 钎料 6061 铝合金钎缝由 α-Al，η-Zn，硅颗粒组成，变质后的 6061 铝合金 Al-Si-Zn 钎缝组织中大块初晶硅消失，产物主要为 α-Al，η-Zn，小块状硅颗粒、AlP 相.

关键词：变质处理；钎焊；6061 铝合金；硅
中图分类号：TG425 **文献标识码**：A **文章编号**：0253-360X(2013)11-0053-04

戴 玮

0 序 言

6061 铝合金的固相线与常规 Al-12Si 钎料的熔点相近，钎焊难度较大，钎焊时母材易发生晶粒长大、熔蚀等现象. 为此研究者们试图开发出低熔点钎料来取代常规 Al-12Si 钎料. 向 Al-12Si 合金中添加适量的铜，可以降低钎料熔点[1-3]，但大约 20% 的铜加入才能使钎料熔点降至 530 ℃附近. 然而大量 Cu 元素的加入使得钎缝塑性下降，接头强度降低. Ni，RE 等元素虽然能优化 Al-12Si 合金组织，但对于钎料熔点的影响不明显[4]. 还有一部分学者尝试将温度较低的锌基钎料用于铝合金的钎焊，其中使用 Zn-Al 钎料钎焊的 3003 铝合金接头强度可达 160 MPa[5]. 另外研究还发现向 Zn-Al 钎料中添加适量 Cu 元素有助于提高钎料钎焊接头的力学性能[6]. 然而由于锌在铝合金中有较大的固溶度，钎焊时铝合金母材易出现熔蚀，所以该钎料的应用也受到了限制.

Al-Si-Zn 钎料由于其较高铝含量可以降低熔蚀缺陷，适当的锌含量可以降低钎料熔点的优点，受到研究者的关注[7,8]. 然而由于 Al-Si-Zn 钎料中初晶硅粗大且呈现不规则的块状，共晶硅呈针状，导致钎缝断后伸长率和抗拉强度较低. 因此有必要对其进行变质处理. 已有研究表明，Cu-P 中间合金对过共晶铝硅合金中的初晶硅有良好的变质作用[9]，但在富含锌的 Al-Si-Zn 体系中尚未有类似的报道. 文中采用 Cu-P 中间合金对 Al-Si-Zn 钎料进行变质处理，研究 Cu-P 变质对 Al-Si-Zn 钎料及 6061 铝合金钎缝组织的影响，探讨 Cu-P 合金在富锌体系中对硅的变质机理.

1 试验方法

试验用钎料采用国家标准 GB/T 470—2008《锌锭》Zn99.995(含锌量质量分数不小于 99.995%)，国家标准 GB/T 1196—2008《重熔用铝锭》Al99.90(含铝量质量分数不小于 99.90%)，及 Al-12Si 中间合金铸锭混合熔炼，试验用变质剂为 Cu-8P 合金，分别配制得到的钎料化学成分如表 1 所示. 试验母材为 6061 铝合金，试样规格为 60 mm × 25 mm × 3 mm，化学成分为 Al-0.6Si-1.1Mg-0.25Cu-0.15Mn(质量分数，%)；所用钎剂为 $CsKAlF_4$. 试验之前先用 400 号碳化硅砂布对 6061 铝合金板进行打磨，保持铝合金表面光洁，之后用丙酮去除表面油污，再用 15% 的 NaOH 溶液处理，温度为 50 ~ 60 ℃，时间为 15 s 左右；然后再用清水清洗，再用体积分数为 1∶3 的稀硝酸溶液浸蚀，浸蚀时间约为 10 s 左右，最后依次用清水、乙醇清洗，自然晾干备用. 钎焊接头形式选用对接接头，采用火焰钎焊方式加热形成钎焊接头.

收稿日期：2013-01-28
基金项目：科技部科技人员服务企业行动资助项目(2009GJ20040)

表 1 钎料合金化学成分(质量分数,%)

Table 1 Chemical compositions of filler metals

编号	Si	Zn	Cu-P	Al
1	6.5	42	0	余量
2	6.5	42	0.5	余量
3	6.5	42	1.0	余量
4	6.5	42	1.5	余量
5	6.5	42	2.0	余量
6	6.5	42	2.5	余量

2 试验结果及分析

2.1 Cu-P 添加量对钎焊接头抗拉强度的影响

向钎料中添加不同含量的 Cu-P 中间合金,制备得到 Al-Si-Zn 系列钎料. 用该系列钎料钎焊的 6061 铝合金对接接头力学性能如图 1 所示. 结果表明,当 Cu-P 添加量为 0.5% 时,接头抗拉强度变化很少. 随着钎料中 Cu-P 含量的增加,钎焊接头抗拉强度逐渐提高. 当中间合金含量提高至 1.5% 时,钎缝强度达到最大值 144 MPa. 继续增加中间合金含量,钎料接头强度呈下降趋势. 这是因为较多的 Cu-P 合金加入会在钎缝中生成 Al_2Cu 化合物,降低了 6061 铝合金钎缝的力学性能,并且较高的铜含量还会恶化钎料的耐腐蚀性能[1].

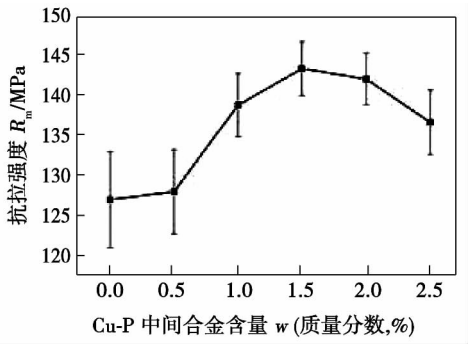

图 1 Cu-P 含量对 6061 铝合金钎焊接头抗拉强度的影响

Fig. 1 Effect of Cu-P content on tensile strength of 6061 alumimum breazed joints

2.2 钎料组织分析

选取抗拉强度最高时的 Cu-P 含量的钎料合金(Cu-P 合金含量为 1.5%)与变质前进行对比,金相组织如图 2 所示. 在未变质的钎料基体中,硅相呈长针状,基体组织粗大,硅相杂乱分布,而变质之后的钎料基体组织细小,分布均匀. 变质前的钎料合金中的初晶硅为块状,共晶硅围绕块状初晶硅呈放射性生长,部分针状相长度可达 500 μm. Al-Si-Zn 中加入 Cu-P 后,小块状初晶硅增多,尺寸减小至 50 μm 以下,形状为规则多边形. 同时变质后钎料中针状共晶硅长度也明显减小,针状共晶硅被"钝化"为短杆状,由此可见,Cu-P 合金变质剂对初晶硅及共晶硅都有良好的变质效果.

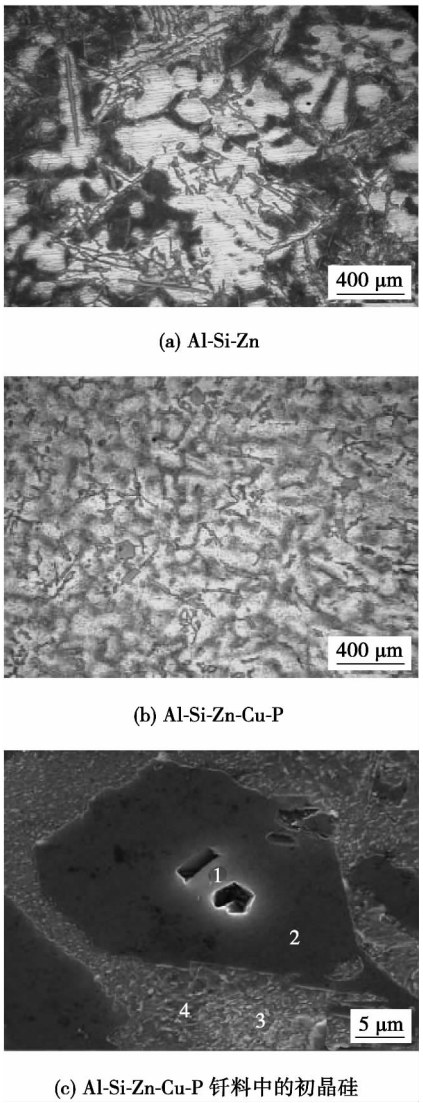

图 2 钎料显微组织形貌

Fig. 2 Microstructure of filler metals

变质之后钎料的物相组成发生了变化. 由于 Cu-P 合金的加入,钎料中出现了 $CuZn_4$ 化合物相(图 3). 初晶硅周围分布的颜色较深的颗粒状相含有约 2.72% 的 Cu 元素,因为铜在铝中的固溶度室温时只有约 0.05%,而铜在锌中的溶解度可以忽略不计. 结合 XRD 分析结果,该相应该为 $CuZn_4$ 相. 细小 $CuZn_4$ 相在钎料基体中均匀分布,避免了硬脆的 Al_2Cu 相生成造成的钎料发脆、加工性能极差的现象. 对初晶硅附近区域进行能谱分析,结果见表 2. 初晶硅的中心部位有明显的 P 元素富集,根

据文献[9],磷的变质机理为生成 AlP,并且作为初晶硅的异质形核核心存在,细化硅晶粒. P 元素在高硅铝合金中对初晶硅同时存在促进形核和抑制生长的作用. 变质处理之后,初晶硅的尺寸大约为 50 μm 左右. 由于 AlP 的出现,初晶硅更加容易依附于该相生成,使得 Al-Si 共晶点往硅侧发生偏移,共晶硅的数量要比变质前少.

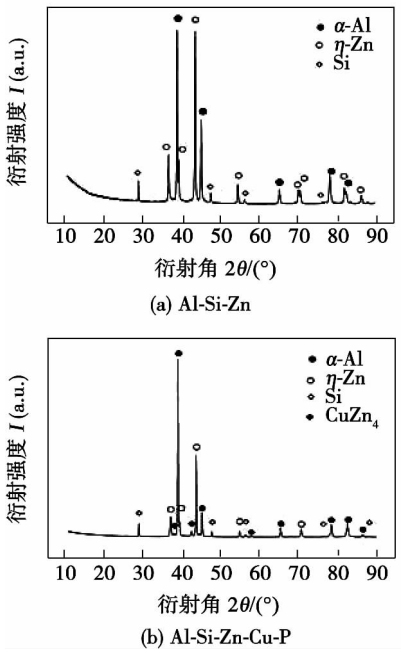

图 3　钎料的 XRD 衍射图谱

Fig. 3　XRD patterns of filler metals

表 2　图 2 中典型相能谱(质量分数,%)

Table 2　EDS results of typical phases in Fig. 2

编号	Zn	Al	Si	P	Cu
1	1.95	6.51	88.74	2.79	—
2	0.78	2.12	97.10	—	—
3	27.64	71.45	0.92		—
4	54.81	42.47	—	—	2.72

2.3　钎焊接头组织分析

分别使用 Al-Si-Zn 钎料及 Al-Si-Zn-Cu-P 钎料对 6061 铝合金进行钎焊试验,所得的钎缝微观组织如图 4 所示. 变质前后的钎料钎焊的 6061 铝合金接头都可以看到较为清晰的界面结构,并且由该界面向钎缝内部生长出笋状的铝基固溶体,该笋状固溶体的存在是钎缝实现良好连接的基础. 此外 Al-Si-Zn 钎缝中有少量初晶硅出现,共晶硅呈现长条状围绕初晶硅呈放射状生长. 添加磷铜合金变质之后,钎缝中无初晶硅出现,共晶硅尺寸变小,由长针状转变为短棒状.

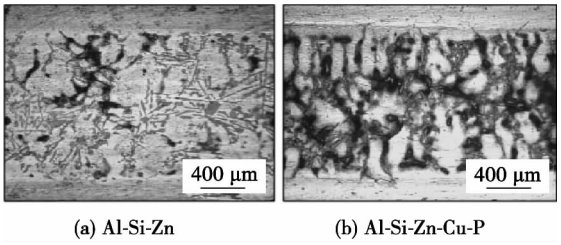

图 4　6061 铝合金钎缝组织形貌

Fig. 4　Microstructure of 6061 aluminum brazing seam

变质前后的 6061 铝合金钎缝的 XRD 图谱如图 5 所示. 变质之后 $CuZn_4$ 相在钎缝中消失. 钎焊过程中,钎料及母材发生了互扩散. 由于铝与锌有较大的固溶度,母材中大量的 Al 元素进入钎缝,抢夺了钎料中原有的 $CuZn_4$ 相中的 Zn 原子,使其固溶进铝固溶体中. 6061 铝合金中 Mg 元素的含量为 1.1%,随着钎焊扩散时铝母材与钎料的互扩散,母材中的 Mg 元素也扩散进入了钎缝中,将有可能与钎料中失去 Zn 原子的 $CuZn_4$ 相反应形成含有 Cu 元素与 Mg 元素的新相.

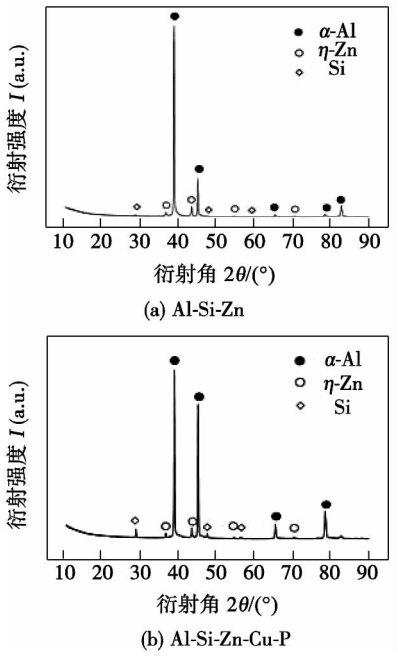

图 5　6061 铝合金钎缝 XRD 衍射图谱

Fig. 5　XRD patterns of 6061 aluminum brazed seam

对 Al-Si-Zn-Cu-P 钎料 6061 铝合金钎缝的显微组织通过 SEM 进行观察,典型的形貌如图 6 所示,钎缝内部无明显大块初晶硅出现,且共晶硅也呈现出短棒状. 硅相周围为深色的基体(图 6 中点 6),根据能谱分析,该相铝含量为 72.88%,为 α-Al 固溶体,在 α-Al 中还固溶有较多的 Zn 及 Si 元素. 钎缝

基体上分布有网格状的浅灰色相(图6中点7),表3中的能谱结果表明该相主要成分为 Zn 和 Al 元素,并且含 1% 硅及 2.69% 铜,该处为 α-Al 与 η-Zn 的共析体. 点5及点8能谱分析结果中均有 Mg 元素出现. 由于 Al-Si-Zn 钎料在钎焊过程中呈现液态,大大提高了 Mg 元素在其中的扩散速率,所以在钎缝内部能发现这种含有 Cu 元素与 Mg 元素的相.

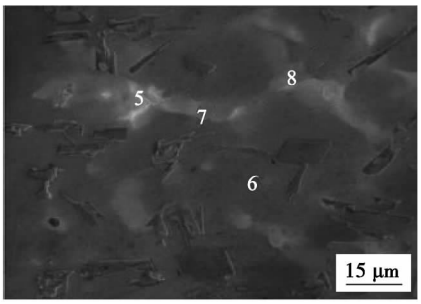

图6 6061 铝合金 Al-Si-Zn-Cu-P 钎缝内部形貌

Fig. 6 SEM of 6061 aluminum alloy brazed joint with Al-Si-Zn-Cu-P filler metal

表3 图6中典型相能谱(质量分数,%)

Table 3 EDS results of typical phases in Fig. 6

编号	Zn	Al	Si	Cu	Mg
5	81.75	8.36	—	4.92	4.97
6	25.14	72.88	1.98	—	—
7	68.95	27.27	1.08	2.69	—
8	86.07	6.07	—	4.31	3.54

3 结 论

(1) 采用 Cu-P 变质后的 Al-Si-Zn 钎料对 6061 铝合金进行钎焊,接头抗拉强度在 Cu-P 合金添加量为 1.5% 时达到最大值 144 MPa.

(2) Cu-P 变质之后钎料组织中初晶硅被细化,共晶硅由长针状变为短棒状. 钎料主要由 η-Zn,α-Al,Si,AlP 及 $CuZn_4$ 组成,AlP 作为初晶硅的异质形核核心,细化了初晶硅颗粒.

(3) Cu-P 变质后 Al-Si-Zn 钎料 6061 铝合金钎缝产物主要为 α-Al,η-Zn 与 α-Al 的共析体,硅和 AlP. 钎焊时母材中的 Mg 元素与 Cu 元素能够通过扩散进入钎缝.

参考文献:

[1] Chang S Y, Tsao L C, Li T Y, *et al*. Joining 6061 aluminum alloy with Al-Si-Cu filler metals [J]. Journal of Alloys and Compounds, 2009, 488(1): 174 - 180.

[2] 朱 宏,薛松柏,盛 重. 合金元素对6063铝合金阶梯焊中温钎料性能的影响 [J]. 焊接学报, 2009, 30(8): 33 - 36.
Zhu Hong, Xue Songbai, Sheng Zhong. Effect of alloying elements on intermediate temperature filler metal in stepped welding of 6063 aluminum alloy [J]. Transactions of the China Welding Institution, 2009, 30(8): 33 - 36.

[3] Shi Yaowu, Yu Yang, Li Yapeng, *et al*. Study on the microstructure and wettability of an Al-Cu-Si braze containing small amounts of rare earth erbium [J]. Journal of Materials Engineering and Performance, 2009, 18(3): 278 - 281.

[4] Zhang Guowei, Bao Yefeng, Jiang Yongfeng, *et al*. Microstructure and mechanical properties of 6063 aluminum alloy brazed joints with Al-Si-Cu-Ni-RE filler metal [J]. Journal of Materials Engineering and Performance, 2011, 20(8): 1451 - 1456.

[5] Dai Wei, Xue Songbai, Lou Jiyuan, *et al*. Torch brazing 3003 aluminum alloy with Zn-Al filler metal [J]. Transactions of Nonferrous Metals Society of China, 2012, 22(1): 30 - 35.

[6] 王 辉,何思渊,褚旭明,等. Zn-Al-Cu 基合金无钎剂钎焊泡沫铝的界面结构及力学性能 [J]. 金属学报, 2009, 45(6): 723 - 728.
Wang Hui, He Siyuan, Chu Xuming, *et al*. Interfacial structure and mechnical properties of alumnium foam joints fluxless-soldered with Zn-Al-Cu base alloy [J]. Acta Metallurgica Sinica, 2009, 45(6): 723 - 728.

[7] 戴 玮,薛松柏,蒋士芹,等. 6061 铝合金中温钎焊接头组织与性能 [J]. 焊接学报, 2012, 33(5): 105 - 108.
Dai Wei, Xue Songbai, Jiang Shiqin, *et al*. Microstructures and mechanical properties of 6061 Al joints brazed with a low-melting point filler [J]. Transactions of the China Welding Institution, 2012, 33(5): 105 - 108.

[8] Suzuki K, Kagayama M, Takeuchi Y. Eutectic phase equilibrium of Al-Si-Zn system and its applicability for lower temperature brazing [J]. Light Metal, 1993, 43(10): 533 - 538.

[9] Zhang Henghua, Duan Haili, Shao Guangjie, *et al*. Microstructure and mechanical properties of hypereutectic Al-Si alloy modified with Cu-P [J]. Rare Metal, 2008, 27(1): 59 - 63.

作者简介: 戴 玮,男,1986 年出生,博士研究生. 主要从事铝合金钎焊技术研究. 发表论文 10 篇. Email: dave_d_w@126.com

通讯作者: 薛松柏,男,教授,博士研究生导师. Email: Xuesb@nuaa.edu.cn

Abstract: Based on the Nastac model, a new capture mechanism, named node-based-correction method, was proposed to improve cellular automaton (CA) technique in the simulation of grain growth during solidification process with arbitrary crystallographic orientations. By coupling with the finite volume method (finite volume method, FVM), a FVM-CA simulation model was put forward and applied to the simulation of microstructure evolution of solidification during the arc deposition. The influences of the deposition rate on dendrite arm spacing and the growth direction were also discussed. Experiments were carried out to verify the validity of the numerical model. This research will lay the theoretical foundation of the prediction and control of microstructure in additive manufacturing.

Key words: finite volume method; cellular automaton; solidification simulation; macro-micro coupling; grain growth

Joint characteristics of refill friction spot welding of magnesium/aluminium dissimilar metals FENG Xiaosong[1], GUO Lijie[1], MIAO Yugang[2], HAN Duanfeng[2] (1. Shanghai Aerospace Equipments Manufacturer, Shanghai 200245, China; 2. College of Shipbuilding Engineering, Harbin Engineering University, Harbin 150001, China). pp 41 - 44

Abstract: Experiments of refill friction spot welding of Mg/Al dissimilar metals were carried out. The mechanical properties and microstructure of the joints were tested and analyzed. The results showed that the weld spots had smooth appearance and high shear strength, and the shear stress could reach 1 865 kN at the proper welding parameters if the lap joints were properly designed. Little cavity and microcracks are found on the nugget/Mg vertical interface, where is the fracture zone. At the horizontal nugget/Al interface with certain thickness, where the microhardness is obviously higher than that of two-side materials, which has some relation with the formation of brittle and hard intermetallics.

Key words: refill friction spot welding; dissimilar metals; mechanical properties; microstructure

Friction welding of $Zr_{41}Ti_{14}Cu_{12.5}Ni_{10}Be_{22.5}$ bulk metallic glass bar CHEN Biao[1,2], SHI Tielin[1], LIAO Guanglan[1], ZHANG Shuaimou[3] (1. State Key Laboratory of Digital Manufacturing Equipment and Technology, Huazhong University of Science and Technology, Wuhan 430074, China; 2. Department of Mechanical and Electrical Engineering, Hubei University of Education, Wuhan 430205, China; 3. Department of Mechanical Engineering, Anhui Technical College of Mechanical and Electrical Engineering, Wuhu 241000, China). pp 45 - 48

Abstract: A new friction welding system was developed to join the bulk metallic glass. The $Zr_{41}Ti_{14}Cu_{12.5}Ni_{10}Be_{22.5}$ bulk metallic glass bars were joined by this welding system. The welded sample was tested by scanning electron microscope, X-ray diffraction, Vickers hardness and transmission electron microscope. The results show that no incomplete fusion or obvious defects are found, and the welded joint maintains the amorphous structure. The hardness is enhanced because a few nanocrystallines occur in the joint. Subsequently, the friction welding temperature field was simulated using finite element software ANSYS. The simulation results indicate that the friction time can not exceed 0.25 s and the upset forging should be carried out. The temperature on center interface exceeds the glass transition temperature of $Zr_{41}Ti_{14}Cu_{12.5}Ni_{10}Be_{22.5}$, and the superplastic deformation occurs. It is concluded that the new friction welding system can be used to join the bulk metallic glass bars. The simulation results of temperature field accords well with that of the experiment, which is beneficial to optimize the welding parameters and guide the experiment.

Key words: friction welding system; bulk metallic glass; joining; simulation

Impact of addition of Sn on resistivity and solderability of Zn4Al3Cu solder ZHAO Kuaile[1], DU Ning[2], YAN Yanfu[3], LI Chenyang[1] (1. Zhengzhou Coal Mining Machinery Group Co., Ltd., Zhengzhou 450013, China; 2. Zhengzhou Linda Compressor Co., Ltd., Zhengzhou 450000, China; 3. College of Materials Science & Engineering, Henan University of Science & Technology, Luoyang 471003, China). pp 49 - 52

Abstract: The resistivity and solder abilities of Zn4Al3Cu*x*Sn solder alloy were investigated by adding Sn (0 - 15%) into Zn4Al3Cu alloy through alloying principle. Results show that the resistivity of the Zn4Al3Cu*x*Sn solders is reduced with the increasing of the addition of Sn. The resistivity of the Zn4Al3Cu15Sn solder is 7.9×10^{-7} Ω·m which is approximately 47.0% lower than that of the matrix solder. When the content of Sn is lower than 10%, the spreading area of the Zn4Al3Cu*x*Sn solder alloy is increased linearly. The spreading area of Zn4Al3Cu10Sn reaches to the maximum value of 98.3 mm^2, which is about 59.1% larger than that of the matrix solder. It is mainly related to the formation of the new SnZn eutectic phase and the metal intermetallic compounds between the solder and the substrate. Therefore, for the consideration of resistivity and spreading property of the novel solders, the proper addition of Sn is about 10%.

Key words: Zn4Al3Cu solder; resistivity; spreading area

Microstructure of Al-Si-Zn filler metal and brazed seam modified with Cu-P DAI Wei[1], XUE Songbai[1], SUN Bo[2], LOU Jiang[2], WANG Shuiqing[2] (1. College of Materials Science and Technology, Nanjing University of Aeronautics and Astronautics, Nanjing 210016, China; 2. Zhejiang Xinrui Welding Material Co., Ltd., Shengzhou 312452, China). pp 53 - 56

Abstract: The effect of Cu-P modification on the microstructure of Al-Si-Zn filler metal and 6061 aluminum brazed joints were investigated. Experimental results showed that the tensile strength of 6061 aluminum brazed joints were improved by Cu-P addition, and the highest value was achieved at 144 MPa when the content of Cu-P was 1.5%. A small amount of P addition can modify the primary Si and refine α-Al in the filler metal. Primary Si growth based on the finely AlP phases were induced by Cu-P addition, and the size of primary Si was much smaller than that without P. Meanwhile, after P addition, the eutectic

point of Al-Si moves to the Si side. It can be found that the phases in Al-Si-Zn brazed 6061 aluminum joint are α-Al, η-Zn, and Si particles, and the phases in Al-Si-Zn-Cu-P brazed seam are α-Al, η-Zn, fine Si particles, AlP phase.

Key words: modification; brazing; 6061 aluminum alloy; Si

Design of high power underwater laser cutting nozzle

XU Liang[1], WANG Wei[1], LI Xiaoyu[1], XU Yujun[1], LIU Shaowei[2] (1. Harbin Welding Institute, China Academy of Machinery Science and Technology, Harbin 150028, China; 2. Shenyang Xinle Aerospace Co., Ltd., Shenyang 110034, China). pp 57 - 60

Abstract: According to the principle of the laser spot size requirement and the design principle of Laval nozzle, the part of stable section, contraction section, throat section and expansion section of the nozzle were designed. The size of stable section is mainly limited by the overall size of the laser cutting gun. Contraction section is used to connect the stable period and the throat section by using tangent arc transition. In order to ensure the laser go smoothly through the throat, throat diameter must be greater than the laser spot diameter. Expansion section adopts linear expansion method, in view of the cutting seam width limit, divergence angle should not be too large. According to the design size, the supersonic Laval nozzle was manufactured, the jet velocity and stiffness of oxygen flow was improved. In underwater laser cutting experiment, using the local drainage method and larger oxygen flow, 30 mm thick carbon steel plate was cut smoothly. Compared with the convergent nozzle, the cutting effect of the supersonic nozzle has been obviously improved

Key words: underwater; cutting; laser; nozzle

Effect of rare earth Ce on microstructure and properties of Zn-22Al filler metal

WANG Bo[1], LIU Han[1], XUE Songbai[1], LI Yang[1], LOU Jiyuan[2], LOU Yinbin[2] (1. College of Materials Science and Technology, Nanjing University of Aeronautics and Astronautics, Nanjing 210016, China; 2. Zhejiang Xinrui Welding Material Co., Ltd., Shengzhou 312452, China). pp 61 - 64

Abstract: The effects of the rare earth Ce on the resistivity, melting temperature, spreadability, microstructure of Zn-22Al filler metal and shear strength of brazed joints were studied. The results indicated that the addition of Ce has little effect on the resistivity and the melting temperature of the filler metal. But with the addition of Ce, the spreadability is significantly improved, the microstructure is refined obviously. It has been found that Ce can improve the shear strength of Cu/Al joint notablely. When the content of Ce is 0.05%, the spread area of filler metal on Al and Cu substrates reached maximum values, respectively, which are 21.4% and 11.6% higher than those of Zn-22Al alloy respectively. Moreover, the shear strength of Cu/Al joint brazed with Zn-22Al-0.05Ce reaches the peak value of 91.3 MPa, which is improved by 30.3% compared with the joint brazed with Zn-22Al alloy. However, with the addition of excessive amount of Ce, some brittle Ce-bearing phases appear in the microstructure and their sizes increase, and the spreadability of filler metal and shear strength of Cu/Al joint deteriorate significantly.

Key words: rare earth Ce; Zn-Al filler metal; spreadability; microstructure; mechanical properties

Microstructure and mechanical properties of MIG welded joint of laser melting deposited TA15 titanium alloy

DU Borui, TIAN Xiangjun, WANG Huaming (School of Material Science and Engineering, Beihang University, Beijing 100191, China). pp 65 - 68

Abstract: Laser melting deposited (LMD) TA15 and rolled TA15 were welded by argon arc welding. The microstructure and phase constitution of the welded joint were studied by optical microscopy and scanning electron microscopy. The microhardness and mechanical properties of the welded joint were tested. The results indicate that the weld zone (WZ) mainly consists of columnar crystals with thick lamellar structure which epitaxially grow from the substrates. The grains in heat affected zone (HAZ) of rolled TA15 grow seriously because of its sensitivity to heat. The columnar grains in HAZ near weld zone of LMD TA15 turn into equiaxial grains. The microhardness of HAZ of LMD TA15 is the highest, while the WZ and HAZ of rolled TA15 is the lowest. The tensile strength of the welded joint is lower than that of both base metals, but the plasticity corresponds to the rolled TA15. Fracture position locates in the HAZ of rolled TA15.

Key words: titanium alloy; laser melting deposition; argon-arc welding; microstructure; mechanical properties

Fatigue life prediction of transverse cross welded joint based on different S - N curve

FAN Wenxue[1,2], CHEN Furong[1], XIE Ruijun[1], GAO Jian[1] (1. School of Materials Science and Engineering, Inner Mongolia University of Technology, Hohhot 010051, China; 2. School of Mining Institute, Inner Mongolia University of Technology, Hohhot 010051, China). pp 69 - 72

Abstract: Three kinds of S - N curves including experimental S - N curve, experience S - N curve and standard S - N curve were established by MSC. Fatigue software. The effects of residual stress, average stress and joint shape were considered. And these curves were revised according to the related criterion and used to predict the fatigue life of Q235B cross-shaped welded joint. The results show that, the fatigue damage locations of welded joint is consistent with that of experiment by S - N curve method based on MSC. Fatigue. The deviation is 7.9%-28% between the prediction values of experiment S - N curve and that of standard S - N curve. The deviation is 3.3%-19% between the prediction values of experiment S - N curve and that of experience S - N curve. The prediction values of experience S - N curve are higher than that of experiment S - N curve and that of standard S - N curve is more conservative.

Key words: cross welded joint; fatigue life; finite element analysis; S - N curve

Filler wire melting dynamics during laser beam welding with filler wire

LIU Hongbing[1], TAO Wang[2,3], CHEN Jie[1], YANG Zhibin[2], CHEN Lei[1], ZHAN Xiaohong[1], LI Liqun[2] (1.